doi:10.1016/S1525-0016(02)00061-8

Genetic Redox Preconditioning Differentially Modulates AP-1 and NFκB Responses Following Cardiac Ischemia/Reperfusion Injury and Protects against Necrosis and Apoptosis

Jusan Yang,[1,3] Jennifer J. Marden,[3] Chenguang Fan,[3] Salih Sanlioglu,[2] Robert M. Weiss,[2,4] Teresa C. Ritchie,[1,3] Robin L. Davisson,[1,3] and John F. Engelhardt[1,2,3,*]

[1]*Department of Anatomy & Cell Biology,* [2]*Department of Internal Medicine,* [3]*The Center for Gene Therapy of Cystic Fibrosis and Other Genetic Diseases, and* [4]*Iowa City VA Medical Center, University of Iowa College of Medicine, Iowa City, Iowa 52242*

**To whom correspondence and reprint requests should be addressed. Fax: (319) 335-7744. E-mail: john-engelhardt@uiowa.edu.*

Reactive oxygen species have been established as key mediators of cardiac injury following ischemia/reperfusion (I/R). We hypothesized that superoxide formation at different subcellular locations following cardiac I/R injury may differentially regulate cellular responses that determine pathophysiologic outcomes. Recombinant adenoviruses expressing Cu/ZnSOD or MnSOD were utilized to modulate superoxide levels in the cytoplasmic or mitochondrial compartments, respectively, prior to coronary artery I/R injury in the rat heart. Ectopic expression of both MnSOD and Cu/ZnSOD afforded protection from I/R injury, as evidenced by a significant reduction in serum creatine kinase levels, infarct size, malondialdehyde levels, and apoptotic cell death in comparison to controls. MnSOD and Cu/ZnSOD expression also significantly altered the kinetics of NFκB and AP-1 activation following I/R injury, characterized by a delayed induction of NFκB and abrogated AP-1 response. Western blot analysis of Bcl-2, Bcl-xL, Bad, Caspase 3, PDK1, and phospho-Akt also revealed SOD-mediated changes in gene expression consistent with protection and decreased apoptosis. These findings support the notion that both mitochondrial and cytoplasmic-derived SOD induce changes in AP-1 and NFκB activity, creating an antiapoptotic microenvironment within cardiomyocytes that affords protection following I/R injury.

Key Words: ischemia, reperfusion, apoptosis, heart, infarction, gene therapy

INTRODUCTION

Ischemia/reperfusion (I/R) injury to the heart is a pathophysiologic consequence often associated with several common clinical procedures (e.g., thrombolysis, angioplasty, and coronary bypass surgery). Oxidative stress, caused by the production of excess reactive oxygen species (ROS) during reperfusion, is one of the main mechanisms proposed to explain I/R pathogenesis. The excess formation of ROS, including superoxide anion ($^{\bullet}O_2^-$), hydrogen peroxide (H_2O_2), and hydroxyl radical ($^{\bullet}OH$), following I/R can lead to direct oxidative damage of DNA, mitochondria, proteins, and lipids and contributes to necrosis in the ischemic zone. ROS can also regulate redox-sensitive signal transduction pathways, including NFκB and AP-1, which may be involved in programmed cell death (apoptosis) or in promoting cell survival [1–4]. Both necrosis and apoptosis contribute to the total cell death incurred during I/R, with apoptosis accounting for 50% or more [5,6]. NFκB is known to suppress apoptosis in ventricular myocytes and plays an essential role in ischemic preconditioning in the heart [7,8]. The protective role of NFκB in preconditioning appears to be associated with the induction of Bcl-2, a component of an antiapoptotic pathway [9,10]. However, it is not clear whether AP-1 promotes apoptosis or cell survival [9,11].

Following myocardial I/R, dramatic increases in ROS formation are found in both the mitochondria and the cytoplasm of cardiomyocytes [12]. Superoxide dismutase (SOD), a family of enzymes that catalyze the dismutation of superoxide anions into hydrogen peroxide, has two primary intracellular isoforms: Cu/ZnSOD, localized mainly in the cytoplasm, and MnSOD, which is found in mitochondria [13]. Both Cu/ZnSOD and MnSOD have been reported to protect against cardiac I/R injury in transgenic mice [14,15]; however, the distinct roles of

1525-0016/03 $30.00

doi:10.1016/S1525-0016(02)00061-8

these two isoforms following I/R have been reported in other organ systems [16,17]. For example, in the liver, it has been shown that MnSOD is protective from I/R injury while Cu/ZnSOD is not [17]. Although the ability of MnSOD and Cu/ZnSOD to protect the heart from I/R injury has been previously demonstrated in several model systems [14,15,18,19], the pathophysiologic responses to I/R controlled by superoxide production and modulated by SOD in cardiomyocytes remain unclear.

The development of gene therapy techniques that can deliver ROS-modulating genes to the heart is potentially a very powerful tool both for investigating the molecular events involved in myocardial (I/R) injury and for developing new therapeutic approaches. The current study utilizes recombinant adenoviral vectors, encoding either Cu/ZnSOD or MnSOD, in a rat model of cardiac I/R injury. This approach was used to investigate the relative ability of these two enzymes to protect the myocardium from I/R injury and to determine their effect on the signaling pathways that contribute to cardiac injury or survival.

RESULTS

Recombinant Adenoviral Vectors Mediate Highly Efficient Cu/ZnSOD or MnSOD Transgene Expression in the Rat Heart

To establish the parameters for gene delivery to the heart, we first performed experiments evaluating the efficiency and distribution of GFP transgene expression using an Ad.GFP reporter vector. The optimal gene delivery method utilized brief occlusion of the pulmonary artery and aorta to allow for coronary artery infusion of vector delivered into the left ventricle. This method produced high levels of transgene expression (~80%) in the area at risk (AAR) of our ischemic model that peaked by 7 days and gradually declined 2 weeks after the initial infection (Fig. 1A). The decline in transgene expression at 14–21 days was associated with T cell infiltrates and clearance of virally infected cells (data not shown). Infection of the heart with Ad.Cu/ZnSOD or Ad.MnSOD demonstrated a sixfold increase in SOD transgene expression in the AAR compared to baseline (PBS infusion or Ad.BglII-infected control hearts), as detected by native polyacrylamide in-gel enzyme assays (Fig. 1B). These results demonstrate that adenovirally encoded transgenes can effectively be used to manipulate genetically the majority of the AAR prior to I/R injury.

Recombinant Adenovirally Expressed MnSOD and Cu/ZnSOD Correctly Localize to Their Native Subcellular Compartments in Cardiac Cells

Since a goal of this study was to discern potential functional differences in the I/R response that were facilitated by SOD expression in the mitochondria and cytoplasm, we next sought to confirm that overexpressed Cu/ZnSOD or MnSOD maintained its normal pattern of subcellular localization. To this end, we performed immunofluorescence colocalization studies on a rat cardiac cell line (H9C2) following infection with either Ad.MnSOD or Ad.Cu/ZnSOD. In these studies, expression of human MnSOD in H9C2 cells demonstrated absolute colocalization with a mitochondrial marker (Fig. 2). In contrast, adenovirally expressed human Cu/ZnSOD was detected solely in the cytoplasm and did not colocalize with the mitochondria (Fig. 2). These results demonstrate that Ad.Cu/ZnSOD and Ad.MnSOD can express their respective transgenes in the correct subcellular compartments. Hence, these transgenes can be used to discern how mitochondrial and cytoplasmic superoxides control molecular events following I/R injury in the heart.

Ectopic Expression of Either Cu/ZnSOD or MnSOD Reduces Serum Creatine Kinase (CK) Levels and Malondialdehyde (MDA) Levels in the Heart Following I/R

We next sought to determine whether overexpression of MnSOD and/or Cu/ZnSOD in the heart prior to I/R injury could afford cardiac protection. Two endpoints, serum CK levels and MDA measurement of heart tissue, were used as indexes of necrotic cardiac damage and oxidative stress, respectively. Five groups of animals were evaluated in these studies, including: (1) sham-operated without I/R, (2) PBS-infused with I/R, (3) Ad.BglII-infected with I/R, (4) Ad.Cu/ZnSOD-infected with I/R, and (5) Ad.MnSOD-infected with I/R. Serum CK and MDA levels were evaluated prior to I/R and at 1, 3, and 5 h post-I/R. Results from these studies demonstrated no significant differences between baseline and 1-h post-I/R levels of serum CK among all groups of animals. However, both Ad.Cu/ZnSOD and Ad.MnSOD afforded a significant reduction in serum CK at both 3 and 5 h post-I/R, compared to PBS or Ad.BglII-infected control groups (Fig. 3A). The greatest level of reduction (fivefold) was seen at 5 h post-I/R and was equivalent for both MnSOD and Cu/ZnSOD ($P < 0.001$, $n = 10$ for each group) (Fig. 3A). Results from MDA analysis demonstrated several intriguing findings. First, baseline MDA levels prior to I/R injury were significantly reduced for both Cu/ZnSOD and MnSOD compared to all other groups (Fig. 3B). Second, control PBS-infused and Ad.BglII-infected hearts demonstrated a rise in cardiac MDA levels that peaked at 1 h post-I/R and returned to near baseline levels by 5 h. This rise in post-I/R MDA levels was significantly attenuated by Cu/ZnSOD or MnSOD expression (Fig. 3B). However, MnSOD expression appeared to afford a larger level of protection from post-I/R oxidative stress than Cu/ZnSOD, the difference being most significant at the 3-h post-I/R time point. These findings suggest that although enhanced clearance of superoxides in either the cytoplasm or the mitochondria reduces the oxidative stress in the heart following I/R, mitochondrial-derived superoxides may play a dominant role in post-I/R oxidative stress.

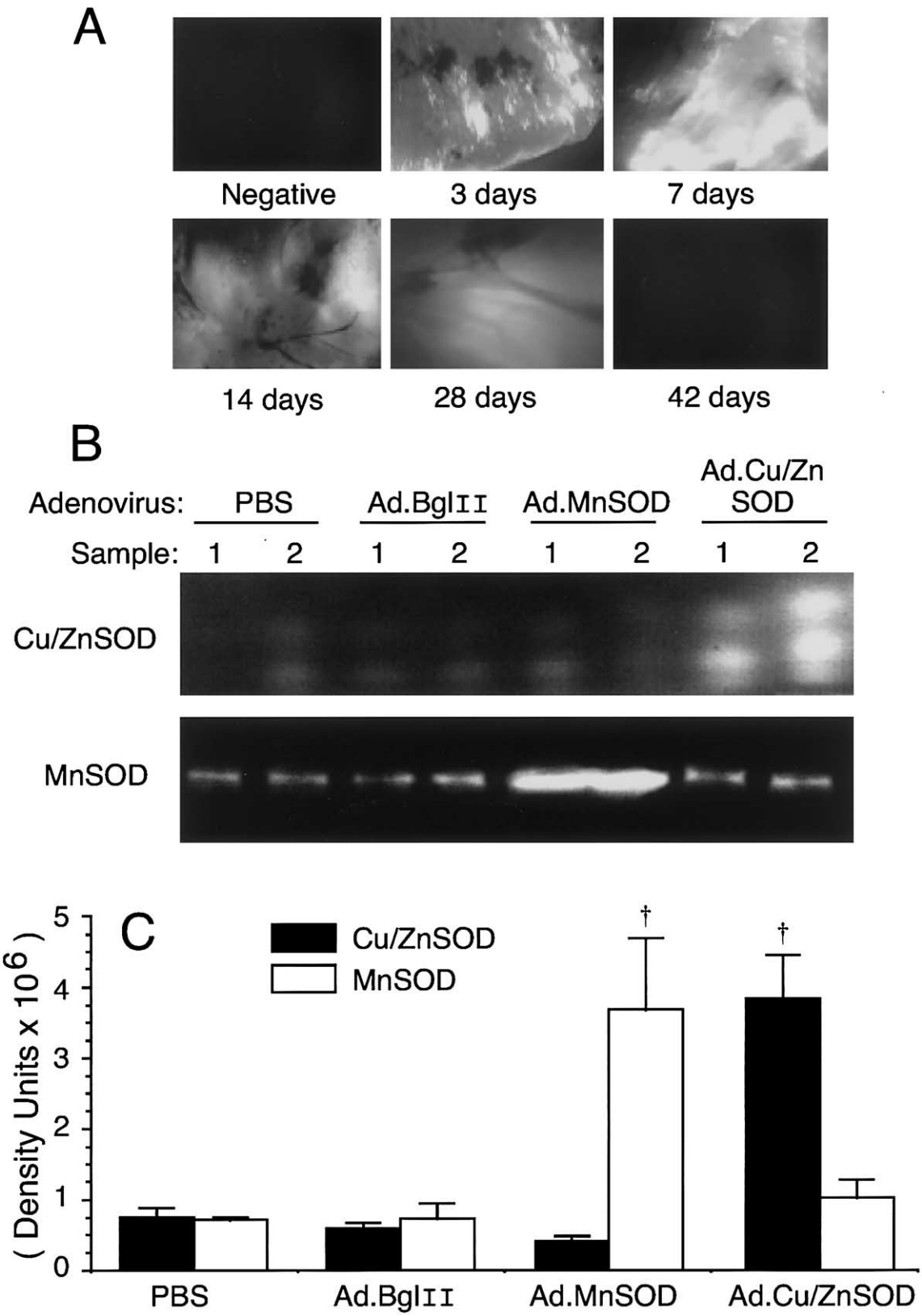

FIG. 1. Recombinant adenovirus-mediated gene transfer to the rat heart. The recombinant adenoviruses Ad.GFP, Ad.BglII, Ad.Cu/ZnSOD, and Ad.MnSOD were instilled into the left ventricle following temporary pulmonary artery and aorta occlusion (2×10^{11} particles in 200 μl). Mock-infected controls included PBS infusion using the same protocol as for adenoviral administration. (A) The time course of eGFP fluorescence as visualized in whole-mount tissue from hearts infected with Ad.GFP. (B) Cu/ZnSOD and MnSOD activities are shown in the top and bottom gels, respectively, for two representative samples in each vector treatment group, as marked above the lanes. All tissues were harvested at 72 h postinfection and animals did not undergo I/R. (C) Quantification of Cu/ZnSOD and MnSOD activity was performed by densitometric analysis of activity gels. Data represent the means (±SEM) of $n = 4$ independent animals in each group. †Statistically significant difference ($P < 0.001$) compared to the PBS or Ad.BglII-infected group using the Student t test.

doi:10.1016/S1525-0016(02)00061-8

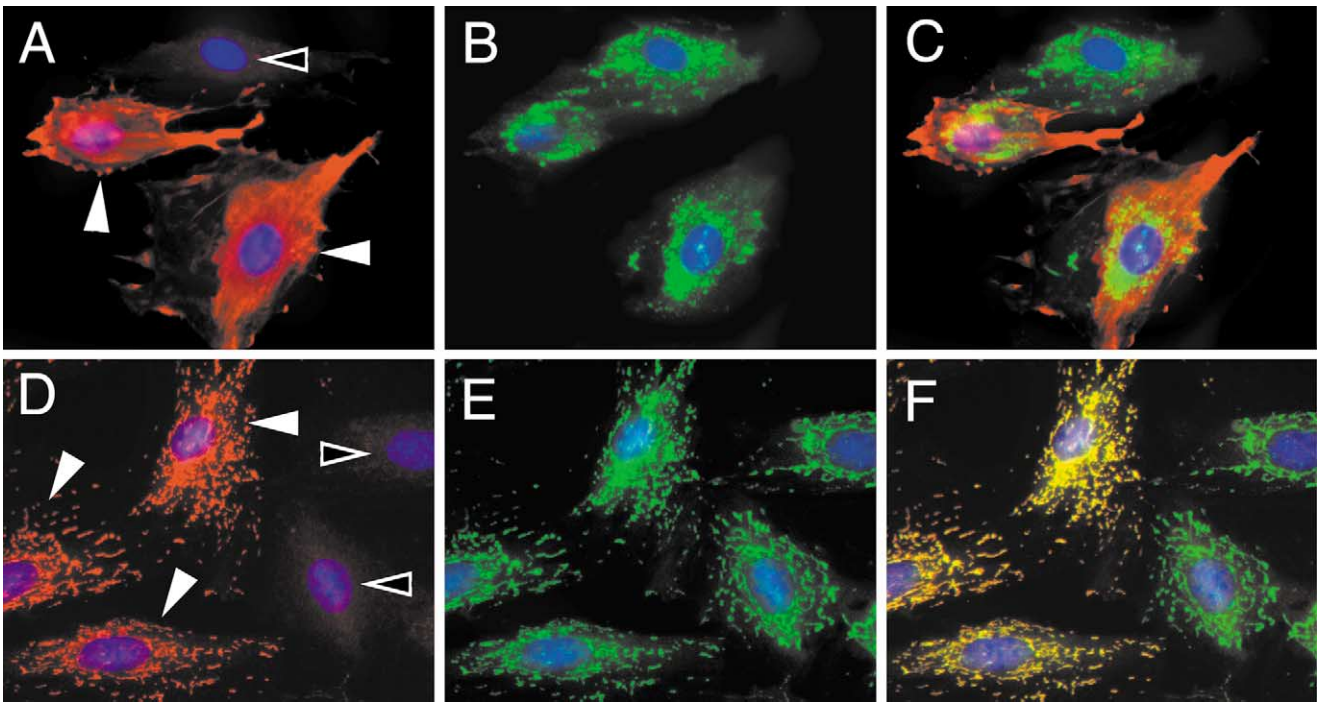

FIG. 2. Recombinant human MnSOD localizes in the mitochondria and recombinant human Cu/ZnSOD localizes in the cytoplasm of rat cardiac cells. H9C2 cells were infected with Ad.Cu/ZnSOD or Ad.MnSOD at an m.o.i. of 1500 particles/cell for 24 h. After fixation and permeabilization, cells were incubated in a sheep anti-human antibody against Cu/ZnSOD or MnSOD. A donkey anti-sheep Alexa Fluor 594 second antibody was used to visualize human Cu/ZnSOD or MnSOD expression (red). MitoFluor green was used to mark the mitochondrial compartment (green) and DAPI was used to counterstain nuclei. Cells infected with Ad.Cu/ZnSOD (A–C) and Ad.MnSOD (D–F) are shown for the various channels. The rhodamine channel depicts positive staining for human Cu/ZnSOD (A) and MnSOD (D). Mitochondria localization (B, E) is shown in the FITC channel. Combined channels (C, F) demonstrate overlap (yellow) of SOD and mitochondrial signals for only Ad.MnSOD-infected cells. Each image contains transgene-positive cells (marked by solid arrowheads), expressing recombinant Cu/ZnSOD or MnSOD, and uninfected negative cells (marked by open arrowheads) that serve as an internal controls for the specificity of staining.

Both Cu/ZnSOD and MnSOD Expression Significantly Reduces Infarct Size Following Cardiac I/R Injury

Infarct size, as determined by Evan's blue and 2,3,5-triphenyltetrazolium chloride (TTC) staining, was used to evaluate the extent of gross structural damage to the heart at both 5-h and 4-day post-I/R time points. Results from these experiments demonstrated that infarct size (as the percentage infarct in the AAR) was significantly reduced (four- to fivefold) at 5 h post-I/R in both Ad.Cu/ZnSOD (17.6 ± 5.1%) and Ad.MnSOD (16.9 ± 7.2%)-infected groups compared to PBS (78.2 ± 11.8%) or Ad.BglII (89.6 ± 9.4%)-infected controls ($P < 0.001$, $n = 10$ for each group) (Figs. 4A and 4C). Similarly, a four- to fivefold reduction in infarct size was achieved in both Ad.Cu/ZnSOD (16.1 ± 2.5%) and Ad.MnSOD (15.2 ± 6.3%)-infected rats compared to PBS (72.4 ± 14.9%) or Ad.BglII (79.3 ± 5.7%)-infected controls at 4 days post-I/R ($P < 0.001$, $n = 4$ for each group) (Figs. 4B and 4D). There was no significant difference in the size of the AAR in the four groups as determined by the relative area of Evan's blue dye exclusion in the heart (Figs. 4C and 4D). These findings suggest that enhanced superoxide clearance in either the cytoplasm or the mitochondria reduces both acute and long-term I/R damage to the heart.

MnSOD or Cu/ZnSOD Expression Attenuates Apoptosis in the Heart Following I/R Injury

Programmed cell death, arising from the activation of proapoptotic signal transduction pathways, reportedly accounts for at least half of the total cell destruction during myocardial I/R [5,6]. It has also been reported that regulation of the cellular redox environment and apoptosis following cardiac I/R are primarily controlled by the mitochondria [20,21]. To this end, we hypothesized that the mechanisms of protection afforded by Cu/ZnSOD or MnSOD overexpression may be different. We reasoned that necrosis (i.e., direct cellular injury), promoted by cytoplasmic superoxide production following I/R, might be more significantly influenced by Cu/ZnSOD expression. In contrast, we hypothesized that MnSOD expression might more significantly attenuate I/R-induced apoptosis. To differentiate between protective effects against necrosis from those affecting apoptosis, we evaluated directly the extent of apoptosis using the TUNEL method. To

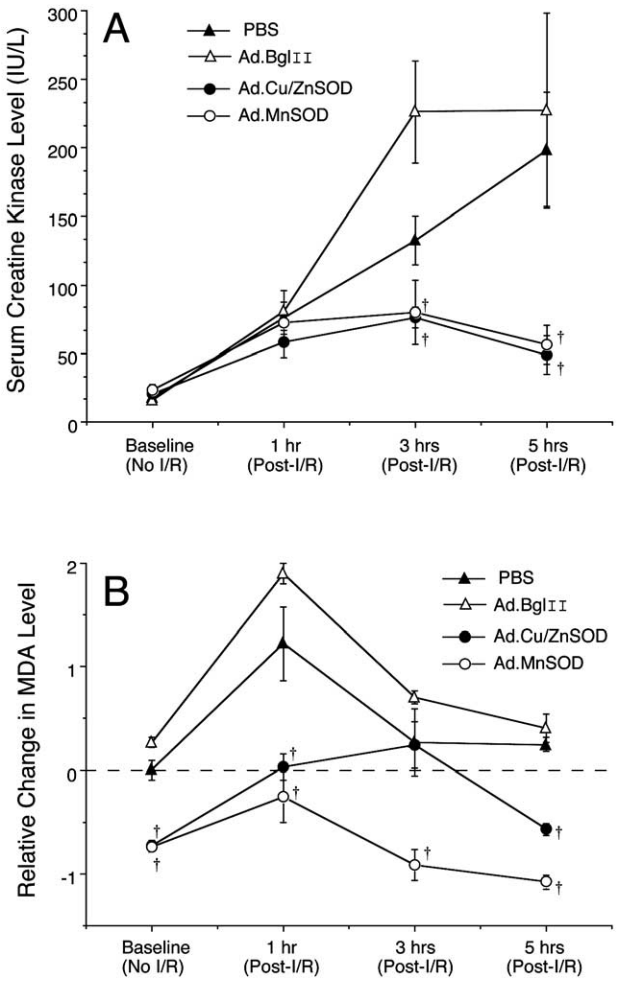

FIG. 3. Expression of Cu/ZnSOD or MnSOD reduces serum creatine kinase and malondialdehyde levels in the heart following I/R injury. (A) Serum samples were assayed for creatine kinase activity in the indicated four experimental groups at the following time points: before I/R and 1, 3, and 5 h post-I/R injury. At the time points of 3 and 5 h post-I/R, both Ad.Cu/ZnSOD and Ad.MnSOD afforded a significant reduction, compared to PBS or Ad.BglII-infected control groups. (B) Tissue samples from the AAR were assayed for MDA activity in the indicated four experimental groups at time points before I/R and at 1, 3, and 5 h post-I/R. The relative changes in MDA levels were assessed in comparison to sham-operated hearts that did not receive I/R injury (baseline MDA levels are indicated by the dotted line). Data represent the means (±SEM) of $n = 10$ independent animals in each group for the CK assay and $n = 4$ independent animals in each group for the MDA assay. †Statistically significant difference ($P < 0.001$) compared to the PBS or Ad.BglII-infected group using the Student t test.

distinguish between potential cell types in the heart that may undergo apoptosis following I/R, we used desmin as a cardiomyocyte-specific marker. We quantified the percentage of cardiomyocytes and other cell types that were apoptotic at 5 h post-I/R in the following five groups: sham-operated no I/R, PBS I/R, Ad.BglII I/R, Ad.Cu/ZnSOD I/R, and Ad.MnSOD I/R. In contrast to our original hypothesis, these studies demonstrated a seven- to ninefold reduction in the percentage of apoptotic cardiomyocytes within the AAR in both Ad.Cu/ZnSOD (1.27 ± 0.62%) and Ad.MnSOD (1.11 ± 0.48%)-infected hearts compared to PBS (8.54 ± 1.44%) or Ad.BglII (10.12 ± 2.32%)-infected controls (Fig. 5). Similar reductions (six- to sevenfold) were seen in the percentage of total apoptotic cells within the AAR in both Ad.Cu/ZnSOD (4.32 ± 2.36%) and Ad.MnSOD (3.87 ± 1.87%)-infected hearts compared to PBS (22.7 ± 4.37%) or Ad.BglII (26.44 ± 5.87%)-infected controls. These results suggest that superoxides in both the cytoplasm and the mitochondria play an important role in apoptotic cell death of cardiomyocytes and other cell types in the heart following I/R injury.

SOD Gene Overexpression Modulates Cardiac NFκB and AP-1 Responses Following I/R Injury

Following I/R injury to the heart, both AP-1 and NFκB are induced at high levels. This is consistent with many reports demonstrating that these signaling pathways are redox regulated [1–4]. To evaluate whether SOD expression was capable of modulating either NFκB and/or AP-1 activity, we performed electrophoresis mobility shift assays (EMSA) on nuclear extracts prepared from AAR tissues following 1 h of ischemia and 1–5 h of reperfusion. Results from these experiments demonstrated that Mn-SOD and Cu/ZnSOD significantly alter the kinetics of NFκB and AP-1 induction. The induction of AP-1 following I/R was blunted and delayed in Ad.Cu/ZnSOD and Ad.MnSOD-infected groups compared to PBS or Ad.BglII-infected controls (Fig. 6). Additionally, AP-1 induction demonstrated a bimodal induction pattern at both 1 and 5 h in controls, but had a single 3-h peak in Ad.Cu/ZnSOD- and Ad.MnSOD-infected groups. In contrast, Cu/ZnSOD and MnSOD expression significantly delayed the induction of NFκB compared to control groups. However, peak levels in Ad.Cu/ZnSOD- and Ad.MnSOD-infected groups at 5 h were similar to those seen in control groups at 3 h post-I/R (Fig. 6). These results suggest that enhanced superoxide clearance in both the mitochondria and the cytoplasm appear to have similar effects on the temporal regulation of NFκB and AP-1 in the acute phases of I/R injury. Furthermore, given the protective effects of SOD expression, the results also suggest a potential link between transcriptional modulation of factors that determine cell fates in the heart following I/R injury.

Overexpression of MnSOD- or Cu/ZnSOD-Regulated Signaling Molecules Involved in Apoptosis and Cell Survival

Bcl-2, Bcl-xL, Bad, and Mcl-1 are among the Bcl-2 family of proteins that regulate mitochondrial-initiated apoptosis and/or cell survival pathways. In contrast, Caspase 3 lies downstream of mitochondria as a primary effector caspase that regulates apoptosis and can also be activated directly by a number of receptor-initiated pathways.

doi:10.1016/S1525-0016(02)00061-8

PDK1 (phosphoinositide-dependent kinase 1), Akt, and PKCε function at cytoplasmic sites and are also known to regulate directly apoptosis, cell survival, and/or NFκB activation. Using Western blotting, we compared the abundance of these mitochondrial and cytoplasmic proteins in control non-I/R hearts and I/R-treated hearts infected with PBS, Ad.BglII, Ad.Cu/ZnSOD, or Ad.MnSOD (Fig. 7A). Quantification in these studies was performed relative to actin as an internal control for protein loading. Significant elevations ($P < 0.05$, $n = 4$ for each group) in phosphoSer473-Akt-1, Mcl-1, Bad, PDK1, Caspase 3, and Bcl-xL were seen in PBS or Ad.BglII-infected animals compared to sham-operated controls. Several notable similarities and differences were seen in the expression patterns of these proteins in Ad.Cu/ZnSOD- and Ad.MnSOD-infected tissues (Fig. 7B). Both Cu/ZnSOD and MnSOD significantly reduced Bad and Caspase 3 expression ($P < 0.05$, $n = 4$ for each group) compared to PBS or Ad.BglII-infected controls. These findings are consistent with the known proapoptotic roles of Caspase 3 and Bad [22] and the reduced apoptosis demonstrated herein with both of these SOD isoforms. Similarly, PDK1 and Bcl-xL were also significantly reduced in both MnSOD- and Cu/ZnSOD-expressing animals ($P < 0.05$, $n = 4$ for each group). Significant increases ($P < 0.05$, $n = 4$ for each group) in phosphoSer473-Akt-1 and Bcl-2 levels were seen in Ad.Cu/ZnSOD- and Ad.MnSOD-infected tissues compared to PBS or Ad.BglII. Ad.MnSOD or Ad.Cu/ZnSOD infection, in comparison to the PBS or Ad.BglII group, invoked no significant alterations in the expression of PKCε or the nonphosphorylated form of Akt-1. Although the trends were similar for both MnSOD- and Cu/ZnSOD-expressing hearts, MnSOD more significantly reduced Caspase 3 and Bcl-xL.

DISCUSSION

Using recombinant adenoviruses to manipulate the redox microenvironment in the mitochondrial and cytoplasmic compartments, the present study has attempted to define more precisely the involvement of superoxides in myocardial I/R injury and their relationship to signaling pathways controlling apoptosis and cell survival. No previous studies have directly compared the efficacy of MnSOD and Cu/ZnSOD overexpression in attenuating cardiac I/R injury. Our findings are in agreement with the protective effects seen in MnSOD- or Cu/ZnSOD-overexpressing transgenic mice [14,15] and adenoviral-mediated MnSOD expression in rat hearts [18,19]. However, in these previous studies, only functional indexes of protection (i.e., postischemic contractility and/or infarct size) from cardiac I/R injury were evaluated. To investigate further the potential mechanisms responsible for MnSOD- and Cu/ZnSOD-mediated protection from I/R injury in the heart, we have evaluated how MnSOD or Cu/ZnSOD expression alters redox-regulated molecular responses to I/R injury that can influence cardiomyocyte survival and apoptosis. We hypothesized that functional differences in MnSOD- or Cu/ZnSOD-mediated protection from cardiac I/R may arise from their distinct subcellular localization and abilities to modulate the redox state of the mitochondria or cytoplasm, respectively. Importantly, our findings confirmed that adenovirally expressed human MnSOD was specifically localized to the mitochondria while overexpression of human Cu/ZnSOD was limited to the cytoplasm. These findings support the correct subcellular partitioning of these adenovirally expressed SOD isoforms in hepatocytes and epithelial cells [17,23,24].

Previous studies using purified SOD and catalase protein have demonstrated that these proteins can significantly reduce the extent of oxidative stress following cardiac I/R as determined by MDA levels [25]. Furthermore, this reduction in I/R-induced MDA by SOD and catalase was correlated with an inhibition of apoptosis. However, in this previous study, SOD and catalase were exogenously applied to *ex vivo* perfused hearts. To investigate whether intracellular expression of MnSOD or Cu/ZnSOD could also protect from I/R-induced oxidative stress, we similarly examined MDA levels in our various experimental groups. Interestingly, nonischemic animals expressing either MnSOD or Cu/ZnSOD in the heart demonstrated a significantly reduced baseline level of MDA compared to PBS-infused or Ad.BglII-infected control hearts. These findings suggest that enhanced clearance of superoxides in either the mitochondria or the cytoplasm can attenuate oxidative stress in nonischemic hearts. Similarly, both MnSOD and Cu/ZnSOD also reduced the peak MDA levels seen in I/R-injured hearts, although MnSOD was slightly more effective. From these studies, we conclude that mitochondria may be a predominant source of redox stress in the heart following I/R injury. Compared to previous studies using exogenously-applied SOD and catalase proteins also capable of reducing I/R-induced MDA accumulation [25], these results suggest that both intracellular and extracellular ROS may play important roles in I/R responses. The observed reduction in oxidative stress afforded by MnSOD and Cu/ZnSOD expression correlated directly with a four- to fivefold protection of the heart from infarct damage at both 5 h and 4 days following I/R. These findings, which for the first time directly compared MnSOD and Cu/ZnSOD, suggest that both SOD isoforms can significantly reduce post-I/R oxidative stress and similarly protect the heart from redox-mediated damage.

Programmed cell death arising from the activation of proapoptotic signal transduction pathways reportedly accounts for at least half of the total cell destruction during myocardial I/R [5,6]. Our studies, demonstrating ~25% total cellular apoptosis and ~10% cardiomyocyte apoptosis in the AAR following I/R-induced injury of vehicle-treated and Ad.BglII-infected animals, are in agreement with these previous findings. In accordance with infarct studies, Cu/ZnSOD or MnSOD expression significantly

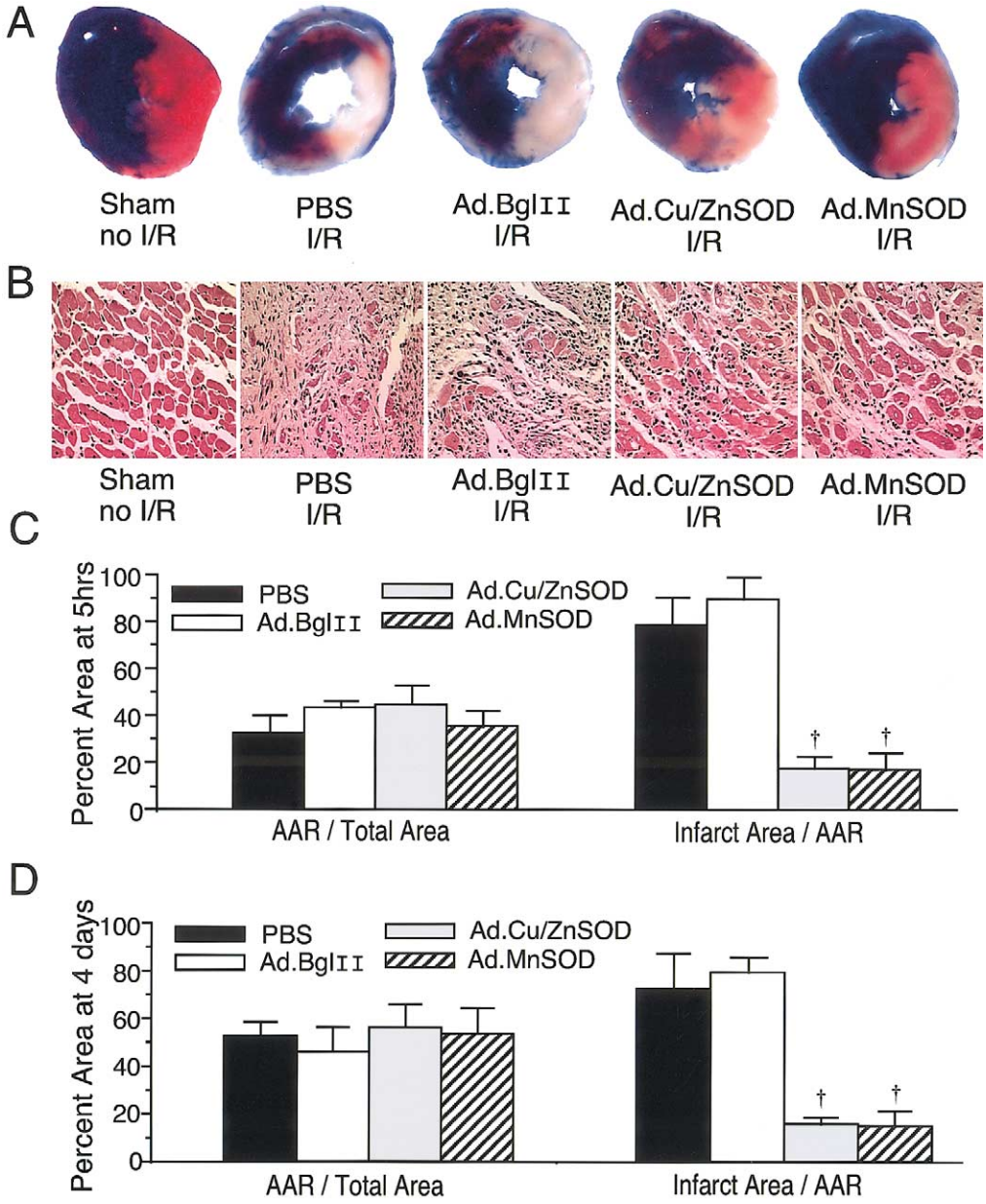

FIG. 4. Expression of either Cu/ZnSOD or MnSOD reduces infarct size following I/R heart injury. Evan's blue and TTC staining was used to demarcate the AAR and infarct zone (see Methods for details). (A) Representative photographs of medial sections of cardiac tissues following Evan's blue and TTC staining of sham-operated no I/R control and at 5 h post-I/R for each of the indicated experimental conditions. (B) Tissue samples in the AAR were examined for histopathology using H&E-stained paraffin sections for each indicated experimental conditions at 4 days post-I/R. Quantitative analyses of Evan's blue and TTC staining to determine the AAR and infarct areas are shown for 5 h post-I/R (C) and 4 days post-I/R (D). The fractional percentage of the infarct area (white regions)/ischemic area (red + white regions) is representative of the extent of damage following I/R injury and takes into account the slight variability in the size of the AAR (non-blue region). Data represent the means (±SEM) for $n = 10$ independent animals in each group for 5 h post-I/R experiments and $n = 4$ independent animals in each group for 4 days post-I/R experiments. †Statistically significant difference ($P < 0.005$) compared to the PBS or Ad.BglII-infected group using the Student t test.

reduced (six- to ninefold) total cell and cardiomyocyte apoptotic death. Based on these findings, we further focused our mechanistic studies on I/R-induced pro- and antiapoptotic signal transduction pathways. We evaluated the activation of two well-known redox-regulated transcription factors, NFκB and AP-1 [26]. NFκB induction appears to be essential for the cardiac-protective effects of ischemic preconditioning [27]. Furthermore, an inverse correlation between changes in NFκB (increased) and AP-1 (decreased) activity following ischemic precondi-

doi:10.1016/S1525-0016(02)00061-8

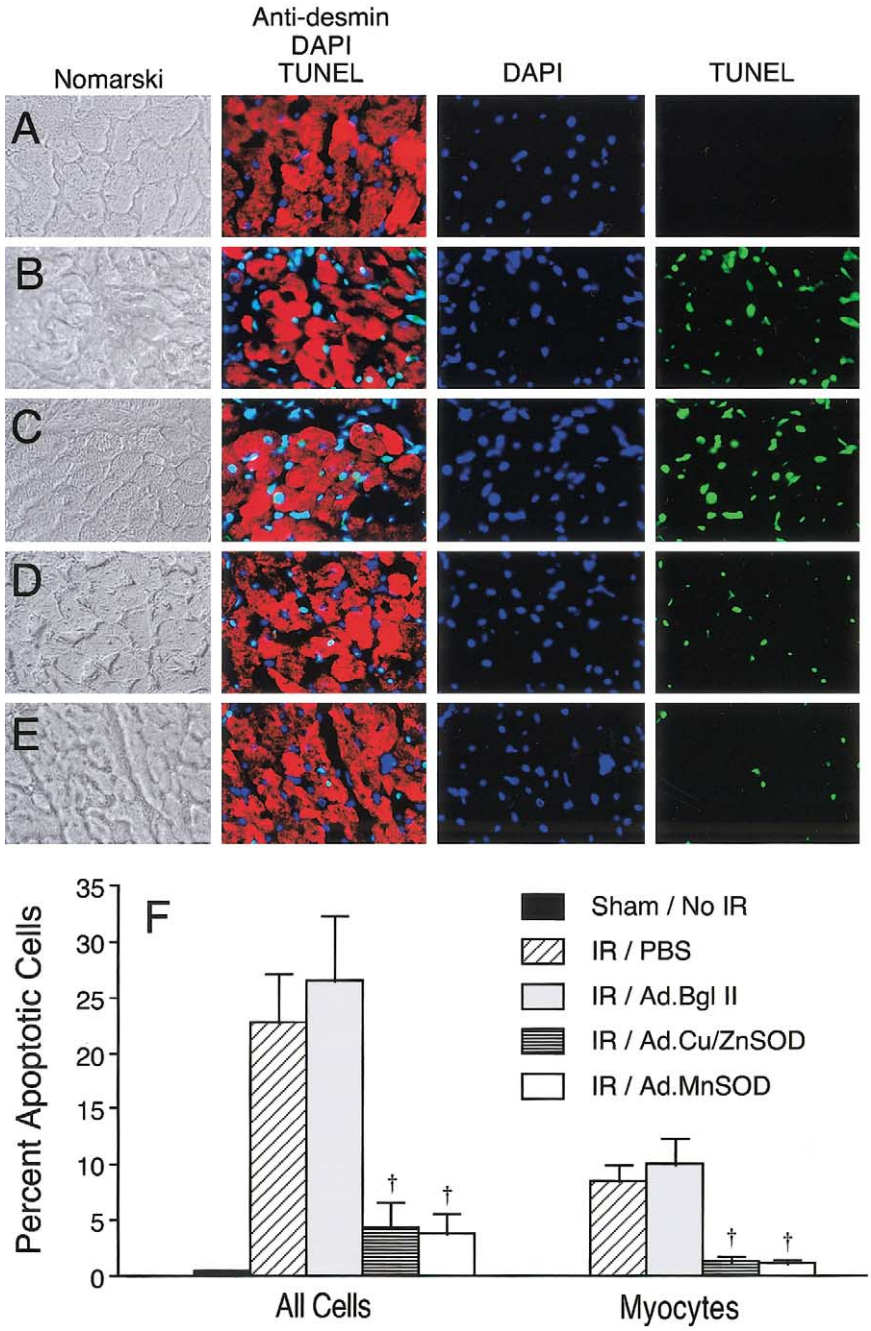

FIG. 5. Ectopic expression of Cu/ZnSOD or MnSOD reduces I/R-induced apoptotic cell death. Combined TUNEL and anti-desmin fluorescence staining was utilized to detect apoptotic cell death at 5 h post-I/R in the following experimental groups: (A) sham operated no I/R, (B) PBS infusion I/R, (C) Ad.BglII-infected I/R, (D) Ad.Cu/ZnSOD-infected I/R, and (E) Ad.MnSOD-infected I/R. TUNEL-positive apoptotic cells appear green, anti-desmin-immunoreactive cardiomyocytes appear red, and DAPI-labeled nuclei of all cell types in the heart appear blue. Each row depicts, from left to right: Nomarski image, combined DAPI/TUNEL/desmin image, DAPI image, and TUNEL image. (F) Quantitative assessment of total apoptotic cells and desmin-positive apoptotic cardiomyocytes in the AAR. For quantification, every other transverse slice of the heart was evaluated for each animal (in total, five transverse tissue slices were analyzed for each heart) and >500 cells were quantified from three sections of each processed transverse slice. Results depict the means (±SEM) of $n = 5$ independent animals in each experimental group. †Statistically significant difference ($P < 0.001$) compared to the PBS or Ad.BglII-infected group using the Student t test.

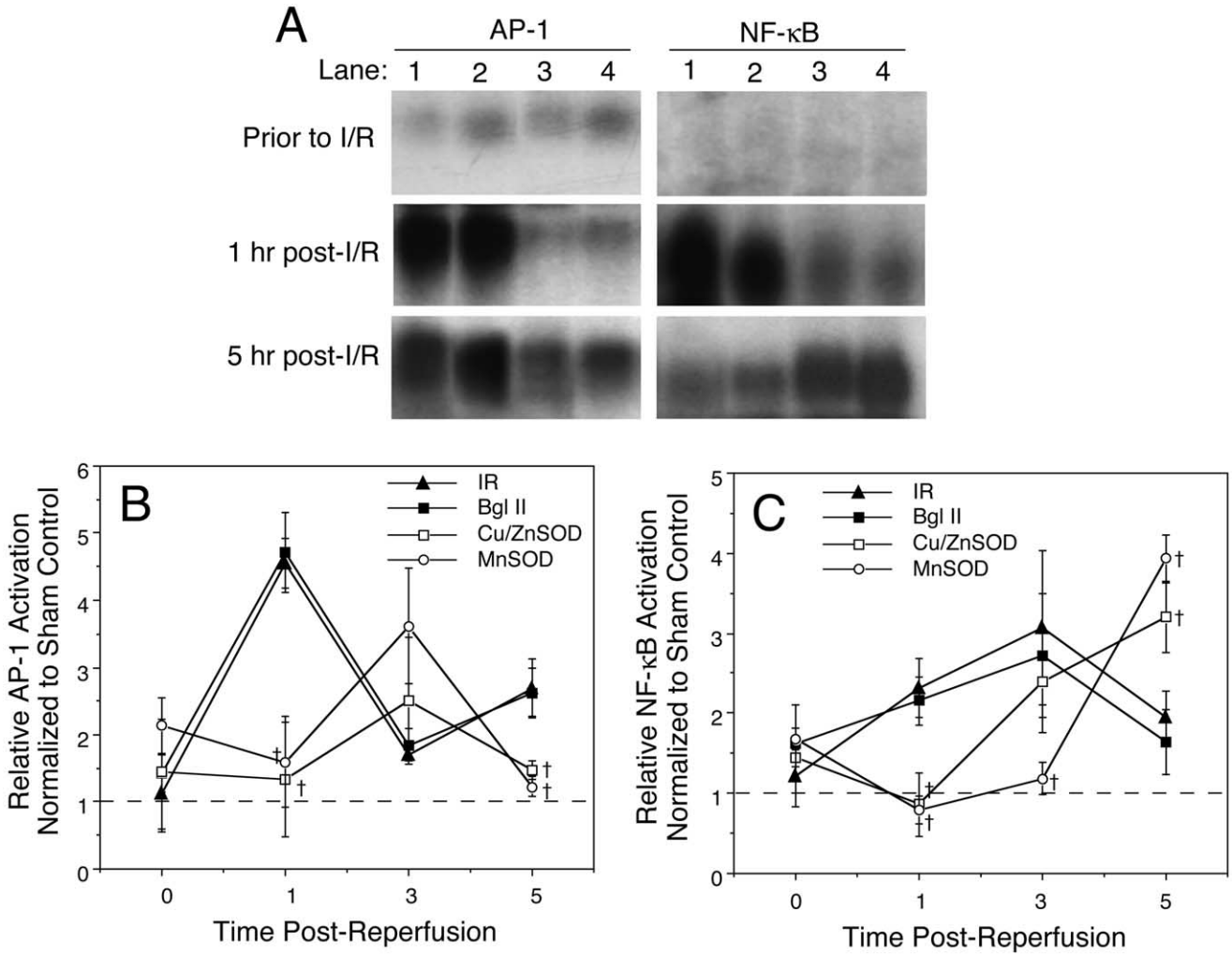

FIG. 6. Ectopic expression of Cu/ZnSOD or MnSOD alters the DNA binding profiles of AP-1 and NFκB following I/R injury. AAR tissue was excised from five experimental groups of animals including sham operated no I/R, PBS-infused I/R, Ad.BglII-infected I/R, Ad.Cu/ZnSOD-infected I/R, and Ad.MnSOD-infected I/R. In the vehicle- and vector-treated groups, four time points were evaluated, including baseline prior to I/R and 1, 3, and 5 h post-I/R. Nuclear extracts were prepared for EMSA of AP-1 and NFκB DNA binding activity. (A) AP-1 (left) and NFκB (right) DNA binding using a ^{32}P-labeled oligonucleotide probe for PBS-infused (lane 1), Ad.BglII-infected (lane 2), Ad.Cu/ZnSOD-infected (lane 3), and Ad.MnSOD-infected (lane 4) hearts at the indicated times on the left. Densitometric quantification of (B) AP-1 and (C) p65/p50 NFκB shifted bands at four time points (before I/R and 1, 3, and 5 h post-I/R) in all four experimental groups. Values are normalized to the average DNA binding seen in sham-operated control untreated hearts ($n = 4$) as denoted by the dashed line. Results depict the mean relative intensities (±SEM) of $n = 4$ animals in each group and time point. †Statistically significant difference ($P < 0.05$) compared to the PBS or Ad.BglII-infected group using the Student t test.

tioning has been hypothesized to regulate transcription of genes (Bcl-2 and p53) that enhance biologic resistance to I/R [11]. In our study, overexpression of either Cu/ZnSOD or MnSOD resulted in a delayed and reduced activation of AP-1 following I/R. Although NFκB activation following I/R was also delayed by Cu/ZnSOD or MnSOD expression, at later time points, its activation was enhanced above that seen in vehicle-treated and Ad.BglII-infected controls. Our findings that the protective effects of MnSOD and Cu/ZnSOD correlate with increased NFκB activity and decreased AP-1 appear to be strikingly similar to findings in ischemic preconditioning models [11,26,27]. This similarity suggests that the protection afforded by MnSOD and Cu/ZnSOD expression may be due to redox-dependent alterations in the temporal regulation of AP-1 and NFκB, which provide a more protective environment that is conducive to cell survival following I/R.

Bcl-2 upregulation in ischemic preconditioned hearts has been associated with protection from cardiac I/R injury [11,26,27] and is thought to be facilitated by increased NFκB activation and decreased AP-1 activation caused by ischemic adaptation [10,11,26]. We therefore investigated whether the level of Bcl-2 and other apoptotic factors might be altered by MnSOD and Cu/ZnSOD

doi:10.1016/S1525-0016(02)00061-8

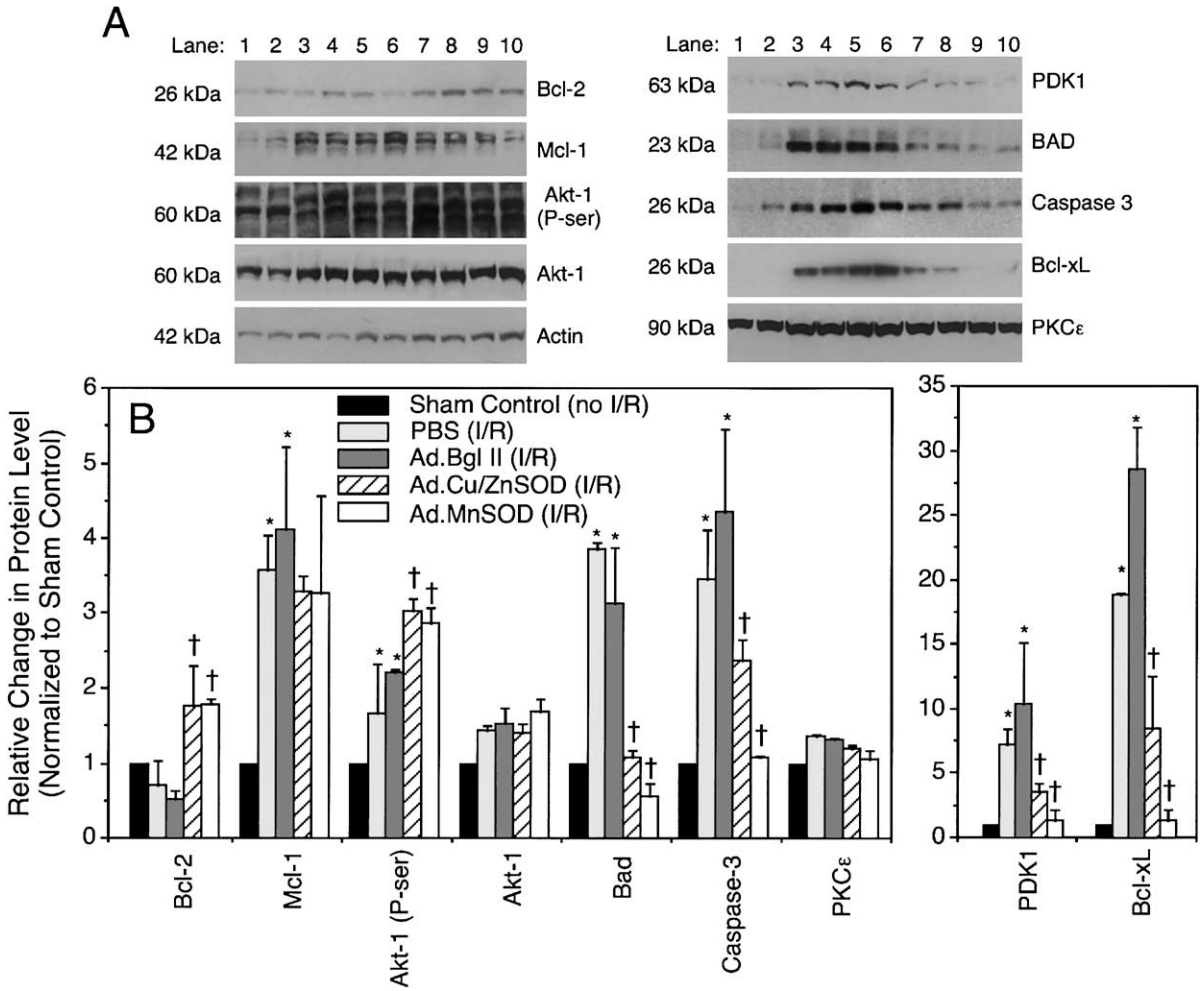

FIG. 7. Ectopic expression of MnSOD and Cu/ZnSOD differentially affects the protein levels of certain apoptotic-related factors. Tissue from the AAR was excised from five groups of experimental hearts and protein extracts were prepared for analysis by Western blot. (A) Representative examples of Western blotting results for eight apoptotic-related factors and an actin internal control as indicated to the right. Lanes 1 and 2, sham-operated nonischemic control; lanes 3 and 4, PBS infused; lanes 5 and 6, Ad.BglII infection; lanes 7 and 8, Ad.Cu/ZnSOD infection; lanes 9 and 10, Ad.MnSOD infection. Duplicate lanes represent independent animals in each group. PBS infusion and all virus-infected groups underwent 1 h of ischemia and 5 h of reperfusion prior to harvest. (B) Densitometric quantification of Western blotting results. Results depict the means (±SEM) of $n = 3$ animals in each group. All groups, except for Akt (nonphosphorylated form) and PKCε, demonstrated significant differences as determined by ANOVA. †Statistically significant difference ($P < 0.05$) compared to the PBS infusion or Ad.BglII-infected group using the Student *t* test. *Statistically significant difference ($P < 0.05$) compared to the nonischemic control group using the Student *t* test. All blots were reprobed for actin as an internal reference for protein loading and all values represent levels normalized to actin signal.

expression. In agreement with the hypothesis that MnSOD and Cu/ZnSOD function similarly as in ischemic preconditioning to protect the heart from apoptotic injury following I/R, we observed significantly enhanced levels of Bcl-2 in hearts expressing both isoforms of SOD. In contrast, vehicle control and Ad.BglII-infected hearts demonstrated a decrease in Bcl-2 expression compared to sham (no I/R) controls, in agreement with previous studies [11]. The finding that NFκB and AP-1 differentially regulate Bcl-2 activity is consistent with our findings that both Cu/ZnSOD and MnSOD induce NFκB and Bcl-2 while reducing AP-1 activation following I/R injury in the heart.

Other apoptotic factors altered by I/R injury in vehicle-injected and Ad.BglII-infected control hearts included a significant upregulation of PDK1, Bcl-xL, Mcl-1, Bad, and Caspase 3 compared to sham-operated control hearts. All of these factors, with the exception of Mcl-1, were significantly reduced by either MnSOD or Cu/ZnSOD expression. Despite these similarities in MnSOD- and Cu/ZnSOD-facilitated alterations in the abundance of apoptotic factors, several subtle differences were observed in the

magnitude of these changes. For example, I/R-induction of Bcl-xL and Caspase 3 was completely abolished by ectopic expression of MnSOD, but not by Cu/ZnSOD. This finding is similar to those demonstrating a decrease in Bcl-xL expression levels in an MnSOD-transfected cell line [28] and suggests differential roles for cytoplasmic and mitochondrial superoxides in controlling Bcl-xL expression. However, since Bcl-xL is recognized as an antiapoptotic factor, the functional significance of MnSOD-induced changes in Bcl-xL expression remains unclear. Another intriguing finding was the significant reduction in PDK1 levels in both Ad.MnSOD- and Ad.Cu/ZnSOD-transduced animals compared to PBS or Ad.BglII-transduced controls. PDK1 is known to mediate the phosphorylation of a number of proteins, including Akt, $p70^{S6}$, kinase, PKA, and PKC [29–31], all of which have been demonstrated to be important in ischemic injury. Furthermore, since constitutively active Akt has been shown to protect cardiomyocytes from hypoxic-induced injury [32], our findings demonstrating increased levels of the phosphorylated active form of Akt in SOD-expressing hearts are in agreement with the decreased levels of apoptosis observed following I/R. Although decreased levels of PDK1 appear to contrast with the increased Akt phosphorylation observed in SOD-expressing hearts, it is important to point out that the absolute level of a kinase does not directly correlate with its activity. Hence, the alterations in the steady-state level of PDK1 must be interpreted in that context.

Both membrane and mitochondria-initiated pathways participate in I/R-induced apoptosis and the generation of ROS [13,33,34]. Our results, demonstrating protection from cardiac I/R injury following ectopic expression of MnSOD or Cu/ZnSOD, substantiate previous findings that illustrated a link between superoxide generation and the control of apoptotic pathways. Using multiple molecular endpoints, our studies demonstrated a striking similarity between MnSOD and Cu/ZnSOD in their ability to modulate AP-1, NFκB, and many apoptotic factors following cardiac I/R, despite their distinct locations within the cell. One potential hypothesis, which might explain how enhanced superoxide clearance in both the mitochondria and the cytoplasm provides similar protective effects, is the notion that mitochondria are the major source of ROS production following I/R that acts on components in the cytoplasm to transduce signals. In such a scenario, MnSOD expression would reduce activation of superoxide-mediated signals by preventing its spread to the cytoplasm. Similarly, in the presence of Cu/ZnSOD expression, superoxides originating from the mitochondria, but acting on factors in the cytoplasm, could also be inhibited. In support of such a hypothesis, regulation of the cellular redox environment and control of apoptosis following cardiac I/R have been suggested to be primarily controlled by the mitochondria [21,35–38]. In contrast, if superoxide production by NADPH oxidase at the cellular membrane is the predominant source of ROS following I/R, one would have expected Cu/ZnSOD expression to be more effective than MnSOD at modulating such an I/R response. Our studies are also consistent with the hypothesis that ROS production is initiated at the cellular membrane and amplified by mitochondria, a scenario also expected to be altered by both MnSOD and Cu/ZnSOD expression. Further investigation into these potential mechanisms of MnSOD and Cu/ZnSOD action following I/R will enhance our understanding of redox-mediated control of apoptosis in the heart and aid in the development of more efficacious therapeutic approaches for ischemic heart disease.

METHODS

Recombinant adenoviruses. Four recombinant E1-deleted adenoviral vectors, Ad.BglII, Ad.GFP, Ad.MnSOD, and Ad.Cu/ZnSOD, expressing their transgenes from the CMV promoter/enhancer, were used in this study. Ad.BglII (empty vector control) and Ad.GFP were both provided by the University of Iowa Vector Core. Ad.MnSOD and Ad.Cu/ZnSOD have been previously described [23]. Recombinant adenoviral stocks were generated as previously described [39] and were desalted by gel filtration in PBS on a Sephadex G-50 column prior to use.

I/R injury model and in vivo adenoviral transduction. Male Wistar rats (250–300 g) were used in a coronary artery ischemia/reperfusion model [40]. Gene transfer with recombinant adenovirus was performed prior to ligature placement around the left anterior descending (LAD) coronary artery. To facilitate gene transfer, the pulmonary artery was clamped, and the aorta was temporarily occluded (~15 s) while 200 μl of recombinant adenovirus vector (total 2×10^{11} particles) was injected into the left ventricle chamber to facilitate coronary artery infusion under high pressure. The number of particles experimentally determined to give maximal gene expression with minimum toxicity as measured by the rise in baseline CK at 3 days post-adenoviral gene transfer to the heart was 2×10^{11} (data not shown). The I/R protocol was performed at 3 days postinfection and included 1 h of coronary artery occlusion, followed by 1, 3, and 5 h or 4 days of reperfusion. Histopathologic examination of ischemic and infarct size was determined using a previously described [41] method to demarcate the AAR and infarct region using Evan's blue dye and TTC staining. Briefly, at the end of postreperfusion, the LAD coronary artery was religated at the same position. Following injection of Evan's blue into the left ventricle, the heart was removed and perfused with 1× PBS at room temperature and then directly frozen *en bloc* in liquid nitrogen for storage at −80°C. At the time of analysis, the heart tissue was warmed in a −20°C freezer for 2 h and sectioned transversely (1 mm), followed by staining in 1% TTC at 37°C for 20 min. To stop the staining, the tissue was rinsed in 10% neutralized formalin for 12 h and then weighed and visualized with a digital camera to determine the fraction of each section with blue, red, or white staining. The AAR was determined as the percentage of red plus white in relation to the total area (red plus white plus blue). Infarct size was determined as the percentage of white compared to the total area of white plus red. The nonischemic region, ischemic region (AAR), and infarct region were quantified by computer planimetry using NIH Image (v1.62). Calculations were averaged over all sections from each heart, and the contribution of each section was corrected by its wet weight.

ECG monitoring and measurement of serum CK. A Burdick^{M} EK/5A recorder was used for the ECG monitoring during I/R. An elevation or depression (depending on the lead placement) of ST-T waves was taken to indicate experimental ischemia after tightening of the coronary ligature. Normalization of ST-T waves indicated experimental reperfusion after the sutures were released. These two criteria were used for all animals to ensure

doi:10.1016/S1525-0016(02)00061-8

proper functioning of the occluding and releasing sutures. Serum CK levels were measured using a kit following the manufacturer's instructions with modifications (Sigma–Aldrich, St. Louis, MO). Blood samples (~50 μl) were collected via the tail vein prior to ischemia and post-I/R, and the serum was collected by centrifugation. Ten microliters of serum was dispersed into 96-well microplates, followed by the addition of 250 μl of the A/B reagent mixture. The plate was then moved to a prewarmed sample chamber in a microplate reader (Molecular Devices, Sunnyvale, CA). After 3 min of incubation and mixing, readings were made at 1, 2, and 3 min. The CK serum levels were calculated based on the rate of change in the OD.

Spectrophotometric assay for MDA. The concentration of MDA in the heart tissues was used as an indicator for oxidative stress. MDA was measured using the Bioxytech MDA-586 kit (Oxis Research, Portland, OR) following the manufacturer's protocols with the following modifications. Briefly, 100 mg of heart tissue from the ischemic area (AAR as marked by exclusion of Evan's blue dye perfusion) was homogenized in 300 μl of ice-cold lysis buffer containing 0.05% deoxycholic acid, 0.1% Triton X-100, 5 mM butylated hydroxytoluene in 0.9% NaCl. Sample homogenates were then centrifuged at 3000*g* for 10 min at 4°C and the supernatant was used for subsequent assays. Protein concentration was determined using the Bradford method. One milligram of protein from each sample was mixed with 210 μl of lysis buffer and 5.3 μl of concentrated HCl and incubated at 60°C for 80 min. Six hundred eighty microliters of diluted reagent R1 was then added and centrifuged at 13,000*g* for 5 min. The supernatant was transferred to new tubes and incubated with 115 μl of reagent R2 at 45°C for 60 min. The tubes were then centrifuged at 13,000*g* for 5 min. Finally, the supernatant was measured in a spectrophotometer at 586 nm and concentrations of MDA were calculated using standards. The relative change in MDA levels for each experimental groups was assessed in comparison to control sham-operated hearts that did not receive I/R injury.

Terminal transferase UTP nick-end labeling (TUNEL), anti-desmin antibody labeling, and DAPI staining for detection and quantification of apoptotic cardiomyocytes. A triple-fluorescence-based staining was utilized for quantification of apoptotic cells in the heart. These studies utilized anti-desmin antibody staining to mark cardiomyocytes, DAPI staining to mark nuclei, and TUNEL staining to mark apoptotic nuclei. Following I/R injury, transverse sections of the apex to the atrioventricular groove (1 mm thick) were paraffin embedded. Ten-micrometer paraffin sections were dehydrated for antigen retrieval and permeabilized by placement in 10 mM citrate buffer for 60 min at 60°C. Sections were then washed three times in Tris-buffered saline (TBS) and stained for desmin using an anti-desmin antibody (1:50 dilution, monoclonal mouse anti-human desmin; DAKO Corp., Carpinteria, CA) at room temperature for 60 min. A secondary antibody, Alexa Fluor 594 goat anti-mouse IgG (1:50; Molecular Probes, Eugene, OR) was used to visualize the desmin. TUNEL staining was then performed on each section as follows. Fifty microliters of TUNEL mixture, containing TdT and dUTP in reaction buffer, was placed onto each section (Roche Molecular Biochemicals, Basel, Switzerland) and incubated in the dark in a humidified chamber for 60 min at 37°C. After the slides were rinsed three times in TBS, they were mounted with DAPI mounting medium (Vector Laboratories, Inc., Burlingame, CA) to visualize the nuclei. Samples were analyzed by fluorescence microscopy using rhodamine, FITC, and UV channels. Apoptosis was quantified in the AAR from all experimental conditions and classified as percentage apoptotic desmin-positive (i.e., cardiomyocytes) and non-desmin-positive cells using DAPI to demarcate all nuclei in a given field. The numbers of sections analyzed for each sample are given the figure legends.

EMSA and Western blots. Nuclear and cytoplasmic proteins were extracted from the nonischemic and AAR regions of the heart using a kit from Pierce (Rockford, IL). Briefly, 100 mg of heart tissue was homogenized in 500 μl of ice-cold buffer CER I, mixed with 27.5 μl of ice-cold CER II buffer, and incubated on ice for 1 min. The cytoplasmic fraction was collected as the supernatant following centrifugation. The nuclear fraction was collected by resuspending the pellet in 100 μl of ice-cold NER buffer with vortexing and then centrifugation. The Bio-Rad protein assay (Hercules, CA) was used to measure the protein content of each fraction. EMSA was performed as described [17] using 6 μg of nuclear extract and the following nucleotide sequences: NF-κB, 5′-AGTTGAGGGGACTTTC-CCAGGC-3′; AP-1, 5′-CGCTTGATGAGTCAGCCGGAA-3′ (Promega, Madison, WI). For Western blotting, 40 μg of protein from the cytoplasmic fractions derived from the AAR was analyzed as described [17]. Primary antibodies against cell apoptosis/survival-related proteins were purchased from Upstate Biotechnology, Inc. (phosphoSer473-Akt1) and BD Transduction Laboratories (Caspase 3, PDK1, Akt, Bcl-2, Bcl-xL, Mcl-1, PKCε, and Bad). Actin immunoreactivity, detected using an anti-actin antibody (Santa Cruz Biotechnology, Santa Cruz, CA) was used as an internal control for loading. The antibodies were diluted according to the manufacturers' recommendations. Immunoreactivity was visualized using HRP-conjugated secondary antibodies with ECL detection. Bands on Western blots and EMSA were quantified by densitometry using NIH Image software.

Detection of SOD activity in transduced rat hearts. In-gel activity assays were used to evaluate Cu/ZnSOD and MnSOD activity from hearts transduced and infused in PBS or infected with Ad.BglII, Ad.MnSOD, or Ad.Cu/ZnSOD [24]. Briefly, 200 μg of homogenized tissue protein from the AAR was separated in a native acrylamide gel. The gels were stained in SOD activity reaction buffer (2.45 mM NBT, 2.8×10^{-5} M riboflavin, 28 mM TEMED in distilled water) (Sigma). To selectively stain for MnSOD, 0.75 mM NaCN was included in the reaction buffer to inhibit Cu/ZnSOD activity. Enzymatic activity was defined by regions of clearing in a background of black precipitate. The bands were quantified by densitometry using NIH Image software.

Subcellular localization of ectopically expressed MnSOD and Cu/ZnSOD in rat heart cells. Immunofluorescent localization of recombinant Cu/ZnSOD and MnSOD was performed on a rat-heart-derived cell line, H9C2. Cells were infected with Ad.Cu/ZnSOD or Ad.MnSOD at an m.o.i. of 1500 particles/cell. Cells were fixed in 3.7% formaldehyde for 15 min at 37°C at 24 h postinfection. The cells were then permeabilized using 0.2% Triton X-100 for 5 min at room temperature. Following blocking in 20% donkey serum/PBS for 20 min, the slides were incubated in sheep anti-human Cu/ZnSOD or MnSOD antibody (The Binding Site, Birmingham, United Kingdom) for 30 min at room temperature. Antigens were detected by indirect immunofluorescence using 4 μg/ml donkey anti-sheep Alexa Fluor 594 second antibody (Molecular Probes). Mitochondria were then stained in 20 nM MitoFluor Green (Molecular Probes).

Statistical analysis. ANOVA was used to assess significant differences between three or more groups of experimental conditions. The Student *t* test was then used to analyze differences between two groups. A $P < 0.05$ was considered significant for both ANOVA and the Student *t* test. Results are reported as the means ± SEM.

ACKNOWLEDGMENTS

This work was supported by NIH Grants DK51315 (J.F.E.), HL60316 (G.H.), and the Core Center for Gene Therapy P30 DK54759 (J.F.E.) and a fellowship grant from the American Heart Association (J.Y). We gratefully acknowledge the guidance of Dr. Joseph Hill in electrophysiologic studies and Kevin Wyne and Reitu Agrawal for editorial assistance.

RECEIVED FOR PUBLICATION FEBRUARY 12, 2002; ACCEPTED DECEMBER 16, 2002.

REFERENCES

1. Flohe, L., Brigelius-Flohe, R., Saliou, C., Traber, M. G., and Packer, L. (1997). Redox regulation of NF-kappa B activation. *Free Radical Biol. Med.* **22:** 1115–1126.
2. Lo, Y. Y. C., Wong, J. M. S., and Cruz, T. F. (1996). Reactive oxygen species mediate cytokine activation of c-Jun NH2- terminal kinases. *J. Biol. Chem.* **271:** 15703–15707.
3. Piette, J., *et al.* (1997). Multiple redox regulation in NF-kappaB transcription factor activation. *Biol. Chem.* **378:** 1237–1245.
4. Roberts, M. L., and Cowsert, L. M. (1998). Interleukin-1 beta and reactive oxygen species mediate activation of c-Jun NH2-terminal kinases, in human epithelial cells, by two independent pathways. *Biochem. Biophys. Res. Commun.* **251:** 166–172.

5. Kajstura, J., *et al.* (1996). Apoptotic and necrotic myocyte cell deaths are independent contributing variables of infarct size in rats. *Lab. Invest.* **74:** 86–107.
6. Takashi, E., and Ashraf, M. (2000). Pathologic assessment of myocardial cell necrosis and apoptosis after ischemia and reperfusion with molecular and morphological markers. *J. Mol. Cell. Cardiol.* **32:** 209–224.
7. Xuan, Y. T., *et al.* (1999). Nuclear factor-kappaB plays an essential role in the late phase of ischemic preconditioning in conscious rabbits. *Circ. Res.* **84:** 1095–1109.
8. Morgan, E. N., *et al.* (1999). An essential role for NF-kappaB in the cardioadaptive response to ischemia. *Ann. Thoracic Surg.* **68:** 377–382.
9. Maulik, N., Goswami, S., Galang, N., and Das, D. K. (1999). Differential regulation of Bcl-2, AP-1 and NF-kappaB on cardiomyocyte apoptosis during myocardial ischemic stress adaptation. *FEBS Lett.* **443:** 331–336.
10. Hattori, R., *et al.* (2001). An essential role of the antioxidant gene Bcl-2 in myocardial adaptation to ischemia: an insight with antisense Bcl-2 therapy. *Antioxidants Redox Signaling* **3:** 403–413.
11. Maulik, N., Sasaki, H., Addya, S., and Das, D. K. (2000). Regulation of cardiomyocyte apoptosis by redox-sensitive transcription factors. *FEBS Lett.* **485:** 7–12.
12. Flaherty, J. T., and Weisfeldt, M. L. (1988). Reperfusion injury. *Free Radical Biol. Med.* **5:** 409–419.
13. Engelhardt, J. F. (1999). Redox-mediated gene therapies for environmental injury: approaches and concepts. *Antioxidants Redox Signaling* **1:** 5–27.
14. Chen, Z., *et al.* (1998). Overexpression of MnSOD protects against myocardial ischemia/reperfusion injury in transgenic mice. *J. Mol. Cell. Cardiol.* **30:** 2281–2289.
15. Wang, P., *et al.* (1998). Overexpression of human copper, zinc-superoxide dismutase (SOD1) prevents postischemic injury. *Proc. Natl. Acad. Sci. USA* **95:** 4556–4560.
16. Copin, J. C., Gasche, Y., and Chan, P. H. (2000). Overexpression of copper/zinc superoxide dismutase does not prevent neonatal lethality in mutant mice that lack manganese superoxide dismutase. *Free Radical Biol. Med.* **28:** 1571–1576.
17. Zhou, W., *et al.* (2001). Subcellular site of superoxide dismutase expression differentially controls AP-1 activity and injury in mouse liver following ischemia/reperfusion. *Hepatology* **33:** 902–914.
18. Abunasra, H. J., *et al.* (2001). Efficacy of adenoviral gene transfer with manganese superoxide dismutase and endothelial nitric oxide synthase in reducing ischemia and reperfusion injury. *Eur. J. Cardiothoracic Surg.* **20:** 153–158.
19. Woo, Y. J., *et al.* (1998). Recombinant adenovirus-mediated cardiac gene transfer of superoxide dismutase and catalase attenuates postischemic contractile dysfunction. *Circulation* **98:** II255–260; discussion II260–251.
20. Zhang, P., *et al.* (1997). Thioredoxin peroxidase is a novel inhibitor of apoptosis with a mechanism distinct from that of Bcl-2. *J. Biol. Chem.* **272:** 30615–30618.
21. Tanaka, K., *et al.* (1998). Expression of Id1 results in apoptosis of cardiac myocytes through a redox-dependent mechanism. *J. Biol. Chem.* **273:** 25922–25928.
22. Chao, D. T., and Korsmeyer, S. J. (1998). BCL-2 family: regulators of cell death. *Annu. Rev. Immunol.* **16:** 395–419.
23. Zwacka, R. M., Dudus, L., Epperly, M. W., Greenberger, J. S., and Engelhardt, J. F. (1998). Redox gene therapy protects human IB-3 lung epithelial cells against ionizing radiation-induced apoptosis. *Hum. Gene Ther.* **9:** 1381–1386.
24. Zwacka, R. M., *et al.* (1998). Redox gene therapy for ischemia/reperfusion injury of the liver reduces AP1 and NF-kappaB activation. *Nat. Med.* **4:** 698–704.
25. Galang, N., Sasaki, H., and Maulik, N. (2000). Apoptotic cell death during ischemia/reperfusion and its attenuation by antioxidant therapy. *Toxicology* **148:** 111–118.
26. Sasaki, H., Galang, N., and Maulik, N. (1999). Redox regulation of NF-kappaB and AP-1 in ischemic reperfused heart. *Antioxidants Redox Signaling* **1:** 317–324.
27. Maulik, N., *et al.* (1999). Ischemic preconditioning reduces apoptosis by upregulating anti-death gene Bcl-2. *Circulation* **100:** II369–375.
28. Kiningham, K. K., and St Clair, D. K. (1997). Overexpression of manganese superoxide dismutase selectively modulates the activity of Jun-associated transcription factors in fibrosarcoma cells. *Cancer Res.* **57:** 5265–5271.
29. Pullen, N., *et al.* (1998). Phosphorylation and activation of $p70^{s6k}$ by PDK1. *Science* **279:** 707–710.
30. Cheng, X., Ma, Y., Moore, M., Hemmings, B. A., and Taylor, S. S. (1998). Phosphorylation and activation of cAMP-dependent protein kinase by phosphoinositide-dependent protein kinase. *Proc. Natl. Acad. Sci. USA* **95:** 9849–9854.
31. Le Good, J. A., *et al.* (1998). Protein kinase C isotypes controlled by phosphoinositide 3-kinase through the protein kinase PDK1. *Science* **281:** 2042–2045.
32. Matsui, T., *et al.* (1999). Adenoviral gene transfer of activated phosphatidylinositol 3′-kinase and Akt inhibits apoptosis of hypoxic cardiomyocytes in vitro. *Circulation* **100:** 2373–2379.
33. Lambeth, J. D. (2002). Nox/Duox family of nicotinamide adenine dinucleotide (phosphate) oxidases. *Curr. Opin. Hematol.* **9:** 11–17.
34. Chandel, N. S., Trzyna, W. C., McClintock, D. S., and Schumacker, P. T. (2000). Role of oxidants in NF-kappaB activation and TNF-alpha gene transcription induced by hypoxia and endotoxin. *J. Immunol.* **165:** 1013–1021.
35. Vanden Hoek, T. L., Becker, L. B., Shao, Z., Li, C., and Schumacker, P. T. (1998). Reactive oxygen species released from mitochondria during brief hypoxia induce preconditioning in cardiomyocytes. *J. Biol. Chem.* **273:** 18092–18098.
36. Kulisz, A., Chen, N., Chandel, N. S., Shao, Z., and Schumacker, P. T. (2002). Mitochondrial ROS initiate phosphorylation of p38 MAP kinase during hypoxia in cardiomyocytes. *Am. J. Physiol. Lung Cell. Mol. Physiol.* **282:** L1324–1329.
37. Duranteau, J., Chandel, N. S., Kulisz, A., Shao, Z., and Schumacker, P. T. (1998). Intracellular signaling by reactive oxygen species during hypoxia in cardiomyocytes. *J. Biol. Chem.* **273:** 11619–11624.
38. Schonheit, K., Gille, L., and Nohl, H. (1995). Stimulation and modulation of mitochondrial radical generation during reperfusion injury of ischemic hearts. *Transplant. Proc.* **27:** 2821–2822.
39. Dracopoli, N. C., *et al.* (1994). In *Current Protocols in Human Genetics* (A. L. Boyle, Ed.), Vol. 3. Wiley, New York.
40. Himori, N., and Matsuura, A. (1989). A simple technique for occlusion and reperfusion of coronary artery in conscious rats. *Am. J. Physiol.* **256:** H1719–1725.
41. Vivaldi, M. T., Kloner, R. A., and Schoen, F. J. (1985). Triphenyltetrazolium staining of irreversible ischemic injury following coronary artery occlusion in rats. *Am. J. Pathol.* **121:** 522–530.